



Mechanical and microstructural properties of linear friction welded Al-based metal matrix composites

F. Rotundo,

University of Bologna, DIEM, V.le Risorgimento 2, I-40136 Bologna, Italy

L. Ceschini, A. Morri,

University of Bologna, SMETEC Dept., V. le Risorgimento 4, I-40136 Bologna, Italy

G.L. Garagnani, M. Merlin

University of Ferrara, Engineering Department, Via Saragat 1, I-44122 Ferrara, Italy

INTRODUCTION

Aluminium based metal matrix composites (MMCs) offer higher specific stiffness and strength, better wear resistance and greater thermal stability when compared to the corresponding unreinforced alloys [1]. One of the outstanding challenges in the use of these materials concerns their joining, since traditional fusion welding processes generally lead to microstructural defects, also due to the presence of the ceramic reinforcement and, consequently, to a general decrease in their mechanical properties [2]. These problems can be significantly reduced by the use of solid state joining techniques, such as Friction Stir Welding (FSW) [3]. A main limitation of this process, however, could be the severe wear of the pin [4]. This problem could be overcome by using Linear Friction Welding (LFW), in which the bonding of two flat-edged components is achieved through frictional heating, caused by their relative reciprocating motion, under an axial compressive force [5], without using any consumable tool. Linear friction welded joints on a 2124Al/SiC_p composite were already studied by some of the authors in terms of residual stress caused by the process [6]. The aim of this work was to evaluate the effect of linear friction welding on the microstructure and mechanical behaviour of the composite, by hardness, tensile, fatigue and impact tests.

MATERIAL AND EXPERIMENTAL PROCEDURE

The material studied was a composite with a 2124 Al alloy matrix reinforced with 25vol.% of fine (<3 μm) SiC particles (AMC225xe). It was produced by powder metallurgy at Aerospace Metal Composites Ltd (Farnborough, UK). The billets were forged with a deformation ratio of 6:1, to 15 mm thick plates and then naturally aged to the T4 condition.

The welding process was performed at TWI (The Welding Institute, Cambridge, UK) according to the scheme in Fig.1 [6]. Welding parameters were optimized after some preliminary tests (Tab. 1).

The microstructural characterization was carried out by optical (OM) and scanning electron microscopy (SEM) equipped with an energy dispersive spectroscope (EDS). Image analyses were performed on optical micrographs by the @Image Pro-Plus software.

LFW joints were tested without any post-weld heat treatment. HV₃₀ hardness measurements were carried out across the joints. Tensile tests were performed on a servo hydraulic machine, equipped with a 100 kN load cell and a clip on

extensometer. Dog-bone specimens were machined with the tensile axis perpendicular to the welded plane y-z in Fig.1. Axial fatigue specimens (machined according to ISO/TTA2 [7]) were tested under stress control with R=0, 20 Hz sinusoidal waveform, 10^7 cycles set run-out. Statistical data analysis and SNP curve estimation were performed by the maximum likelihood method [8, 9]. Finally, Charpy impact tests were performed at room temperature on a 50 J CEAST pendulum. V-notch specimens were machined, according to ASTM E23 [10], both from the base material and from the LFW joints. The mechanisms of failure of the composite were investigated by SEM analyses of the fracture surfaces.

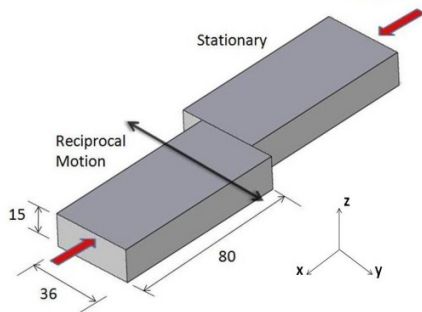


Figure 1: Linear friction welding schematic [6]

Friction/Forge Force	[kN]	100
Pressure	[N/mm ²]	185
Frequency	[Hz]	50
Set Amplitude	[mm]	2
Burn-off	[mm]	2

Table 1: LFW parameters.

RESULTS AND DISCUSSION

Linear friction joints showed the presence of flash material extruded both parallel and normally with respect to the force-motion plane (x-y), as shown in Fig. 2(a). Complete weld penetration was obtained in the MMC joints. The material experienced relevant plastic flow due to the LFW process. None of the typical defects of MMCs arc fusion welding (i.e. TIG and MIG) and excellent particle distribution were found. Three characteristic zones were observed (Fig. 2(b)): Weld centre, where relevant grain refinement occurs, due to concurrent effect of frictional heating and severe plastic deformation; thermo-mechanically affected zone (TMAZ), where the grain orientation follows plastic flow at relatively high temperature; heat affected zone (HAZ), where no plastic deformation occurs, but heating affects the material properties.

No appreciable effect on the reinforcement particle size was observed, in contrast to friction stir welded MMCs [3], due both to the absence of the tool and to the small particle size of the tested composite.

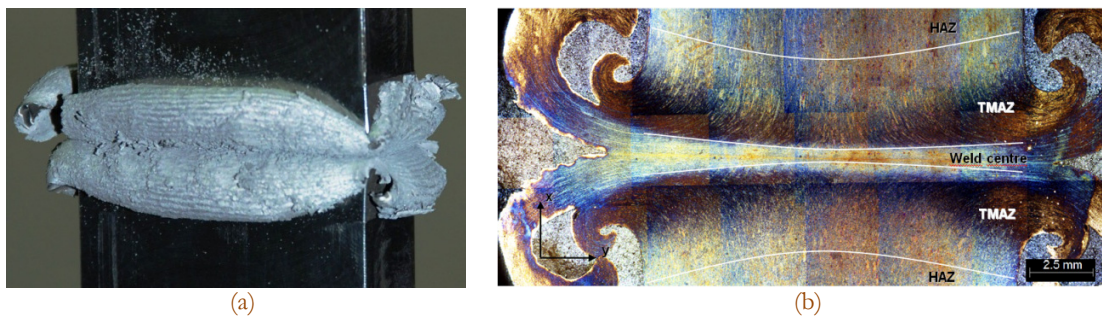


Figure 2: LFW joint shape (a) and etched cross section (b) [9].

As regards to the hardness, the LFW joints showed a minimum value of 194 HV₃₀, at 2 mm from the weld line, whilst 217 HV₃₀ were measured for the base material [9]. Hardness fluctuations were observed along the joint, due to the complex microstructural modifications induced by LFW. The concurrent effects of frictional heating and severe plastic deformation lead to grain refinement and possible modification of the intermetallic phases [3, 9].

Yield strength ($\sigma_{p0.2}$) and ultimate tensile strength were found to be respectively 364 and 562 MPa, with a tensile joint efficiency (the ratio between the joints and nominal base material properties) equal to 78% and 82%, respectively [9]. The elongation to failure (2.4 %) was considerably lower than the base MMC (4.0 %).

The experimental fatigue data and corresponding statistical analysis, with S-N curves at different failure probabilities, are reported in Fig. 3. Fatigue strength at 10^7 cycles was equal to 289 MPa with a 50% probability of failure [9], which is 78% in respect to the fatigue strength of the base material, tested at $R=0.1$ [11].

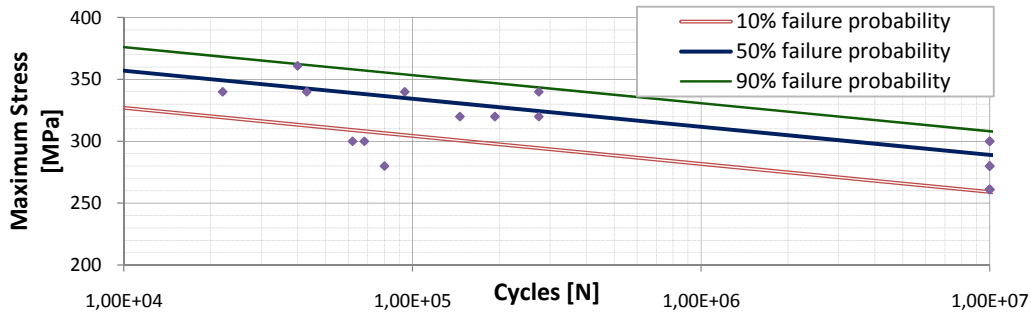


Figure 3: Axial fatigue test data and S-N curves at different failure probability [9].

The average total impact energy of the LF welded composite (1.23 ± 0.21 J) was comparable to that of the base MMC (1.32 ± 0.12 J), with only a slight decrease of about 7%. This is due to the limited modifications that the LFW process caused in reinforcement phase in terms of particles dimension and distribution. Moreover, limited effect were also introduced in the Al matrix, as the microstructure was already extremely fine due to the specific production route, and in the matrix/reinforcement interface.

In the tensile specimens fracture usually occurred in the TMAZ, perpendicularly to the applied load and propagating along the textured zones caused by the process (Fig. 4(a)). The decrease in ductility could therefore be related to the heavily orientated plastic flow characteristic of this zone. SEM analyses of the fracture surfaces (Fig.4(b)) showed a good matrix/reinforcement adhesion, with ductile failure of the Al matrix.

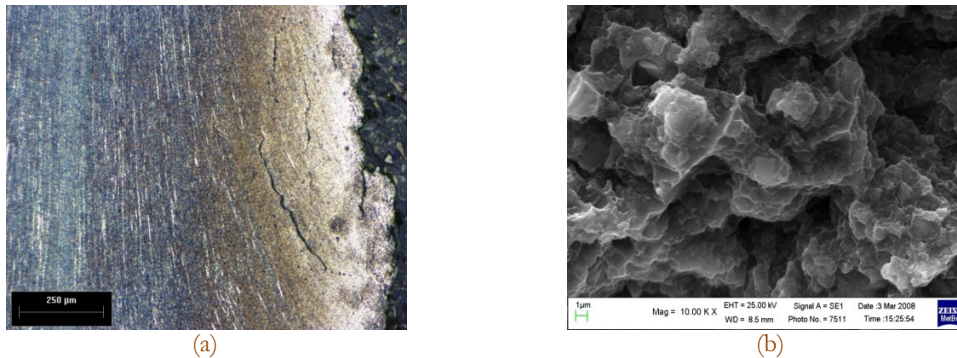


Figure 4: Optical micrographs of a LFW joint showing secondary cracks in the tensile fracture cross section (a) and SEM micrograph of the fracture surface (b) [9].

SEM analyses of the fatigue specimens showed that nucleation sometimes occurred on subsurface at oxide inclusions (Fig. 5(a)). Crack growth, in the area immediately surrounding the initiation site, is tortuous and contains also microscopic cracks and fatigue striations, with a random orientation in the matrix (Fig. 5(b)). As for tensile fracture surfaces, no evidence of interfacial reaction products was detected and only a small amount of fractured particles was present. Traces of ductile failure were also present in the crack growth region (Fig. 13 (b)). Fracture appearance of the overload zone was similar to that of tensile specimens.

CONCLUSIONS

The experimental results demonstrated LFW to be an attractive welding technology for particle reinforced Al-based MMCs. Microstructural analyses showed substantially defect-free joints. Three characteristic zones were identified in the LFW specimens: weld centre, with an ultra-fine microstructure and a uniform particle distribution; thermo-mechanically affected zone (TMAZ) with severe plastic deformation; heat affected zone (HAZ), without visible

microstructural modification to the material. The decrease in hardness was limited to approximately 10% in respect to the base material. The efficiency of the LFW joints was about 80%, in respect to the tensile and fatigue strength (although there was a relevant reduction in the elongation to failure), and 93% in respect to the impact strength. The limited ductility of the LFW specimens could be related to the high fibrosity observed in the TMAZ, where fracture occurred. The analyses of the fracture surfaces evidenced a ductile failure of the Al matrix, without any appreciable matrix-particle debonding or particle cracking.

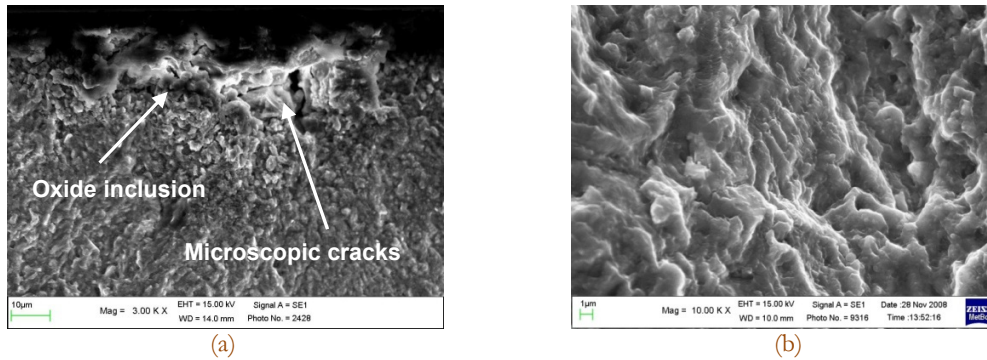


Figure 5: SEM micrographs of oxide inclusion and microscopic cracks in the nucleation zone (a) and crack propagation zone (b) [9].

REFERENCES

- [1] T.W. Clyne, P.J. Withers, *An Introduction to Metal Matrix Composites*, Cambridge University Press (1993).
- [2] M.B.D. Ellis, *Int. Mater. Rev.*, 41(2) (1996) 41.
- [3] L. Ceschini, I. Boromei, G. Minak, A. Morri, F. Tarterini, *Comp. A*, 38 (2007) 1200.
- [4] G.J. Fernandez, L.E. Murr, *Mater. Charact.*, 52 (2004) 65.
- [5] A. Vairis, M. Frost, *Wear*, 217 (1998) 117.
- [6] T.S. Jun, F. Rotundo, L. Ceschini, A.M. Korsunsky, *J. Mater. Design*, (2009) doi:10.1016/j.matdes.2009.10.004.
- [7] ISO/TTA 2. *Tensile tests for discontinuously reinforced metal matrix composites at ambient temperatures*, (1997).
- [8] G. Minak, L. Ceschini, I. Boromei, L. Ponte, *Int. J. Fatigue*, (2009) doi:10.1016/j.ijfatigue.2009.02.018.
- [9] F. Rotundo, L. Ceschini, A. Morri, T.S. Jun, A.M. Korsunsky, *Composites: Part A*, (2010), doi:10.1016/j.compositesa.2010.03.009.
- [10] ASTM E 23. *Standard Test Methods for Notched Bar Impact Testing of Metallic Materials*, (2007).
- [11] www.amc-mmc.co.uk.